The Soil–Precipitation Feedback: A Process Study with a Regional Climate Model

CHRISTOPH SCHÄR, DANIEL LÜTHI, AND URS BEYERLE

Swiss Federal Institute of Technology (ETH), Zurich, Switzerland

ERDMANN HEISE

German Weather Service, Offenbach, Germany

(Manuscript received 29 August 1997, in final form 30 March 1998)

ABSTRACT

Month-long integrations with a regional climate model covering Europe and the Northern Atlantic are utilized to study the sensitivity of the summertime European precipitation climate with respect to the continental-scale soil moisture content. Experiments are conducted for July 1990 and 1993. For each of the two months, the control experiment with the initial soil water distribution derived from the operational ECMWF analysis is compared against two sensitivity experiments with dry and wet initial soil moisture distributions. The results demonstrate that summertime European precipitation climate in a belt ~1000 km wide between the wet Atlantic and the dry Mediterranean climate heavily depends upon the soil moisture content. In this belt, changes in monthly mean precipitation amount to about half of the changes in mean evapotranspiration.

Budget analysis of water substance over selected subdomains demonstrate that the simulated sensitivity cannot be interpreted with the classical recycling mechanism, that is, the surplus of precipitation that falls over wet (as compared to dry) soils does not directly derive from evapotranspiration. Rather, the surplus of precipitation primarily originates from water vapor extracted from the ambient atmospheric flow. Thus, the soil–precipitation feedback must rely on some indirect mechanism, whereby wet soils increase the efficiency of convective precipitation processes.

In order to isolate the physical mechanisms underlying the soil–precipitation feedback, a detailed analysis including an investigation of the mean diurnal cycle throughout the integration period is performed. The key elements of the feedback are the following. First, wet soils (small Bowen ratios) imply the buildup of a comparatively shallow boundary layer. The surface fluxes of heat and moisture are thus concentrated into a comparatively small volume of air, leading to the buildup of high values of low-level moist entropy, thereby providing a source of convective instability. Second, the level of free convection is lowered in the wet experiment, thus facilitating the release of convective instability. Third, the net shortwave absorption at the soil decreases in the wet experiment (as a result of increased cloud cover), but this effect is overpowered by the decrease in net longwave emission (as a result of decreased emission, increased cloud backscatter, and increased water vapor greenhouse effect). Thus the net radiative energy flux is larger in the wet experiments, thereby increasing the moist entropy fluxes into the boundary layer. These three processes act in concert to increase the potential for convective activity.

1. Introduction

Feedback processes between the soil and the atmosphere are of major importance for our climate system. In the extratropics the role of the soils is comparable to that of the oceans. While the oceans store solar energy they receive in summer (and use it to heat the atmosphere in winter), the soils store precipitation they receive in winter (and use it to moisten and cool the atmosphere in summer). The associated seasonal storage of water in the soil introduces long-term memory effects with timescales of several months.

Of particular importance for the soil–atmosphere system are feedback processes by which an increase in evapotranspiration directly or indirectly amplifies precipitation. In this study such effects are referred to as the ''soil–precipitation feedback,'' and herein is meant to apply on a scale of several hundred kilometers. The perception of soil–precipitation feedback effects has changed dramatically in the course of the past 100 years (see Brubaker et al. 1993): Until the late 1930s, the role of the atmosphere in transporting large quantities of moisture over long distances had not properly been recognized. It was often assumed that precipitation would primarily derive from local evapotranspiration. With this simplified view, it appeared straightforward to increase precipitation by artificially increasing local evaporation and transpiration at the expense of runoff. This view lasted until it was realized that the residence time of water molecules in the atmosphere was about one week,

Corresponding author address: Dr. Christoph Schär, Swiss Federal Institute of Technology, GIETH, Winterthurerstr. 190, 8057 Zurich, Switzerland.
E-mail: schaer@geo.umnw.ethz.ch

thus implying that the average water molecule travels by a large distance before it again returns to the earth's surface in the form of falling precipitation. Thus, the simple amplification of precipitation by local evapotranspiration appeared no longer feasible and was heavily criticized as ''evapotranspiration–precipitation fallacy'' (McDonald 1962). This critical view was also supported by estimates of the recycling rate, which did indicate that ''local'' evapotranspiration, even on a continental scale, does often contribute less than 30% to the precipitation amount (Budyko 1974).

Nevertheless, studies with numerical models conducted in the early 1980s detected a strong sensitivity of the precipitation response with respect to evapotranspiration. One of the early studies of this type was that of Shukla and Mintz (1982) who studied the response of a GCM to prescribed sea surface temperatures and soil moisture conditions. Related experiments have in the meantime been performed with a wide range of numerical models. Models were utilized to analyze the global-scale sensitivity to soil moisture conditions (Yeh et al. 1984; Rind 1982), the response to regional soil-moisture anomalies (Rowntree and Bolton 1983), the effect of deforestation (e.g., Dickinson and Henderson-Sellers 1988; Lean and Rowntree 1993), the importance of soil moisture anomalies for episodes of drought and flooding (Oglesby and Erickson 1989; Beljaars et al. 1996; Giorgi et al. 1996), the effects of changes in vegetation (Claussen 1997; Copeland et al. 1996), and the impact of initial soil conditions in weather forecasting models (Mahfouf 1991; Viterbo 1995; Beljaars et al. 1996). Most of these studies noted some increase of precipitation with increasing evapotranspiration, but there are substantial variations depending upon the model, region, and season under consideration. Maximum sensitivity appears to be associated with summertime convective activity in absence of strong synoptic forcing.

There are also a few observational studies on the interannual variability of soil wetness and precipitation that lend support to the hypothesis of an active soil–precipitation feedback. For instance, in a recent observational study of Findell and Eltahir (1997) it is demonstrated that during summer there are statistically significant lag correlations between soil moisture anomalies and subsequent rainfall anomalies over the state of Illinois. Lagged-correlation effects of this type might also be able to explain the anomalous persistence of summertime precipitation in Australia (e.g., Simmonds and Hope 1997) and could give rise to a bimodal distribution of wet and dry seasons under some climatic regimes (Enthekabi et al. 1992).

To reconcile these aforementioned numerical and observational results with the earlier studies about precipitation recycling, it was sometimes argued that the recycling rate according to Budyko's model might underestimate the contribution from nearby evapotranspiration (see Burde et al. 1996). Alternatively, the use of complex parameterization schemes for soil, vegetation, radiation, planetary boundary layer, and convective processes is also questioning the validity of the numerical results (see Enthekabi 1995).

In the current paper the soil–precipitation feedback problem is revisited by means of month-long regional climate model simulations covering Europe. The simulations will be initialized with different soil moisture fields but driven at their lateral boundaries by the same atmospheric forcing. In this way a consistent ensemble of integrations is obtained: All members of the ensemble are characterized by a similar synoptic-scale evolution throughout the month-long integration, while the near-surface climates and hydrological cycles of the individual members of the ensemble are allowed to differ in response to the state of the soil. Our study will confirm that the long residence time of water molecules in the atmosphere precludes any local and direct effect. However, it will also be shown that an indirect effect exists, which allows to reconcile earlier results on precipitation recycling with more recent numerical and observational studies.

The specific motivation for our study is threefold. First, we would like to assess the sensitivity of the summertime European precipitation climate with respect to the continental-scale soil moisture distribution. It is worth noting that many of the pioneering studies on the soil–precipitation feedback have been conducted over the United States or in the Tropics, while comparatively little work was performed for the European regions. The lack of studies covering Europe is surprising and is probably related to the infrequent occurrence of serious drought conditions over most of Europe, rather than to the absence of a soil–precipitation feedback. In fact, one of the pioneering studies carried out over Europe, that of Rowntree and Bolton (1983), revealed a strong sensitivity of precipitation with respect to initial soil moisture conditions.

The second objective of the study is to understand the nature of the feedback process and, in particular, to distinguish between direct and indirect mechanisms. In the direct (or recycling) mechanism, the surplus of precipitation over wet soils derives directly from evapotranspiration within the same region (see Fig. 1a). In contrast, in the indirect (or amplification) mechanism the surplus of precipitation derives from a remote location and is transported over long distances by the atmospheric circulation, but the efficiency of the precipitation processes is determined by the state of the soil (Fig. 1b). The distinction between these two processes depends upon the horizontal scale. In the current study it will be assessed by means of budget considerations on a scale of $\sim$1000 km.

Finally, the third part of the study is dedicated to the isolation and assessment of the mesoscale processes that are relevant for the soil–precipitation feedback processes. In several recent studies (Betts and Ball 1995; Betts et al. 1996) it was suggested that the build up of

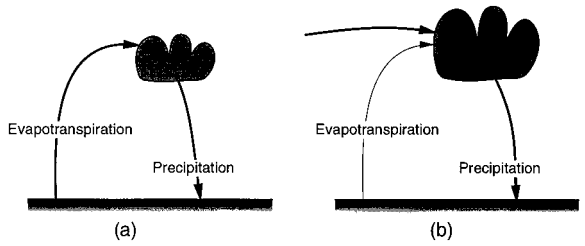

FIG. 1. Two possible mechanisms for the soil–precipitation feedback: According to the recycling hypothesis (a), the surplus of precipitation over wet soils derives primarily from evapotranspiration over the same region. In contrast, in the amplification mechanism (b) it derives from atmospheric transport of water, but the efficiency of the precipitation processes is controlled by the state of the soil.

the daytime boundary layer represents a key to understand the soil–precipitation feedback mechanism. In the current study we will test this theory and also give consideration to radiative feedbacks.

The paper is organized as follows: We start by describing the numerical model and its application in the current study in sections 2 and 3, respectively. Section 4 is devoted to the discussion and validation of the control experiments. The results of the sensitivity experiments are presented in section 5 and are further analyzed in terms of their water budgets and mesoscale dynamical mechanisms in section 6 and 7, respectively. The results of the study are concluded in section 8.

2. Model description

The regional climate simulations performed in this study were undertaken with the mesoscale hydrostatic numerical weather prediction model developed at the German Weather Service (DWD). A detailed description of this model, referred to as ''Europa-Modell'' (EM), is given by Majewski (1991) and DWD (1995). Information on model updates and validation in the operational forecasting practice are given in quarterly reports (DWD 1997). The model was earlier used in a similar setup in previous climate studies (Cress et al. 1995; Lüthi et al. 1996; Schär et al. 1996; Frei et al. 1998).

The horizontal domain utilized in the present series of numerical experiments is shown in Fig. 2. It covers most of Europe and a substantial part of the North Atlantic. Also illustrated in the figure is the model's representation of the earth's topography and several subdomains that will be used for analysis purposes. The model's geometric framework is cast in spherical coordinates with the pole rotated to 32.5°N latitude, 170°W longitude. This rotation of coordinates shifts the computational equator of the grid over Europe, yielding a relatively isotropic horizontal grid. The horizontal resolution is 0.5° (~56 km). In the vertical a hybrid coordinate system is adopted such that at low levels the computational surfaces are terrain following and thereafter transit with height to coincide at upper levels with pressure surfaces. In this way the atmosphere is represented by 20 layers of upward increasing thickness, and a rigid-lid boundary condition is employed at the top of the model domain (i.e., $p = 0$). Further details on the model grid and setup are given in Lüthi et al. (1996).

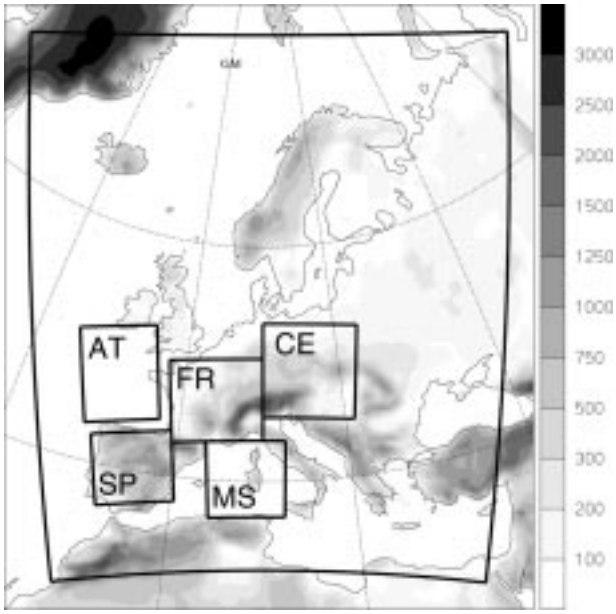

FIG. 2. Computational domain and topography for the current numerical experiments. The analysis domains AT (Atlantic), MS (Mediterranean Sea), SP (Spain), FR (France), and CE (central Europe) are also indicated.

The model's prognostic variables are surface pressure, the horizontal wind components, total heat, and total water content. Total heat and water are converted into temperature, specific humidity, and liquid water content at each time step. The discretization itself is based on finite differencing with a semi-implicit time-stepping scheme employed in conjunction with an Eulerian-based advection scheme. The semi-Lagrangian option was not employed for the current simulations. Blending of the model's fields with the externally specified driving fields is accommodated at the lateral boundaries using the relaxation boundary technique of Davies (1976), which adjust the prognostic variables in a marginal zone. The model is laterally driven by operational ECMWF analysis fields with a 6-h updating frequency.

The parameterized physical processes include a surface layer formulation (Louis 1979) with a prescribed surface roughness length over land and a Charnock-type formulation over the ocean, a boundary layer and turbulence formulation with a second-order closure scheme of hierarchy level 2 (Mellor and Yamada 1974; see also Müller 1981), grid-scale cloud microphysics of Kessler-type including a parameterized ice phase, moist convection formulated as a mass-flux scheme (see Tiedtke 1989), a radiative transfer formulation (Ritter and Geleyn 1992), and a fourth-order horizontal diffusion

scheme. It is to be noted that the adjustment of these schemes based upon the model's performance in an numerical weather prediction mode has helped tune the model appropriate to central European conditions. Several of the aforementioned parameterizations are crucial model components for the current purpose, as will further be discussed in the concluding section.

The model is used with a soil and vegetation formulation of intermediate complexity. Surface temperature is predicted by the extended force–restore method (Jacobsen and Heise 1982), which provides an optimized solution to the heat conduction equation. Three active layers are used to predict the soil water content from appropriate budget relationships, the thicknesses of these layers being 2, 8, and 90 cm, respectively. The heat capacity and diffusivity, as well as several hydraulic parameters (pore volume, field capacity, air dryness point, hydraulic conductivity) and vegetation parameters (wilting point, turgor loss point), are prescribed according to the prevailing soil type (10 types). There is partial coverage with interception and snow storage. Vegetation is prescribed by the fractional plant coverage, the leaf area index, and the root depth. These parameters have a prescribed seasonal cycle, except for the root depth which is kept constant at 70 cm for the current experiments.

Evaporation from the soil comes from three sources. There is potential evaporation from interception storage, bare soil evaporation from the top soil layer over the unvegetated fraction of the soil, and transpiration from all three model layers over vegetated areas. The evaporation rate E_s of bare soil is computed using the assumption $E_s = \min(E_p, F_m)$, where E_p is potential evaporation and F_m the maximum moisture flux through the surface that the soil can sustain (Dickinson 1984).

The computation of plant transpiration E_t basically follows Dickinson (1984). In the version adopted here, energy fluxes between the ground and the plant canopy are neglected, implicitly assuming a vanishing temperature difference between ground and the foliage. Thus the determination of transpiration is reduced to a Monteith (1981) combination formula. Here transpiration mainly depends on the net radiation balance, the bulk transfer coefficient for heat, the saturation deficit of the air, the leaf area index, and the stomatal resistance. In the stomatal resistance r_s all effects mentioned by Dickinson (1984) are included in the following form:

$$r_s^{-1} = r_{\max}^{-1} + (r_{\min}^{-1} - r_{\max}^{-1})(F_{\text{rad}}F_{\text{wat}}F_{\text{tem}}F_{\text{hum}}).$$

We use constant values $r_{\min} = 100$ s m^{-1} and $r_{\max} = 4000$ s m^{-1}. The functions F describe the influence on the stomatal resistance of radiation (F_{rad}), soil water content (F_{wat}), ambient temperature (F_{tem}), and ambient specific humidity (F_{hum}), respectively, and they take the value 1 if optimum conditions are present and the value 0 for unfavorable conditions. The computed transpiration rate is finally reduced by the factor $d_r/(\Sigma\ \Delta z)$, where d_r is the root depth and $\Sigma\ \Delta z$ is the total depth of the active soil layers. As in the present experiments $d_r = 70$ cm and $\Sigma\ \Delta z = 100$ cm; transpiration is confined to 70% of the potential evaporation rate.

The atmospheric data fields for the initial and lateral boundary conditions are derived from ECMWF analysis fields. Details of the associated technical procedures are given in Majewski (1985). At the surface the procedures differ for land and sea grid points. For the former initial fields for soil water content and soil temperature are derived from ECMWF analysis fields with adjustments to account for the different soil types and depths of the two modeling systems. After initialization the soil parameters in the soil layers are predicted. In contrast, for oceanic grid points the sea surface temperature and the distribution of sea ice is updated quasi-continuously from the steering model.

3. Setup of numerical experiments

Month-long regional climate simulations will be presented for July 1990 and July 1993. For each of these months, three experiments are conducted, all of which are driven by the same lateral boundary data. The first experiment is referred to as CTRL and its soil moisture field is initialized at 0000 UTC 1 July from the operational ECMWF analysis. In the two sensitivity experiments exactly the same procedures and the same lateral boundary data are employed, except for an initial adjustment of the initial soil moisture content in the three soil layers. In experiment DRY it is modified by multiplication with a uniform factor 0.5, and in experiment WET by a factor 2. In regions where this procedure yields a water content beyond saturation, the respective part of water is disregarded. Likewise, if the initial soil water in experiment DRY falls short of the air dryness point, the respective amount of water was added to match this minimum value.

The factors 0.5 and 2 used above are motivated by the analysis of the Illinois soil water dataset (Findell and Eltahir 1997). This analysis shows that the interannual variability of summertime soil moisture over Illinois spans a factor of around 2. Since a corresponding study for the European soils is not available to us, it is possible that the current sensitivity experiments span a range larger than that provided by the interannual variability.

Since our model is initialized from a soil moisture field generated by the operational ECMWF land surface scheme, the initialized soil moisture conditions are—even in the CTRL experiment—merely of qualitative nature. It would be advantageous to adapt the initial soil moisture data to the particular soil and evapotranspiration scheme under use. Such a task would require driving our scheme with radiation, precipitation, temperature, and wind data over the months preceding initialization—a task beyond the scope of this study. However, for our purpose to study the soil–precipitation feed-

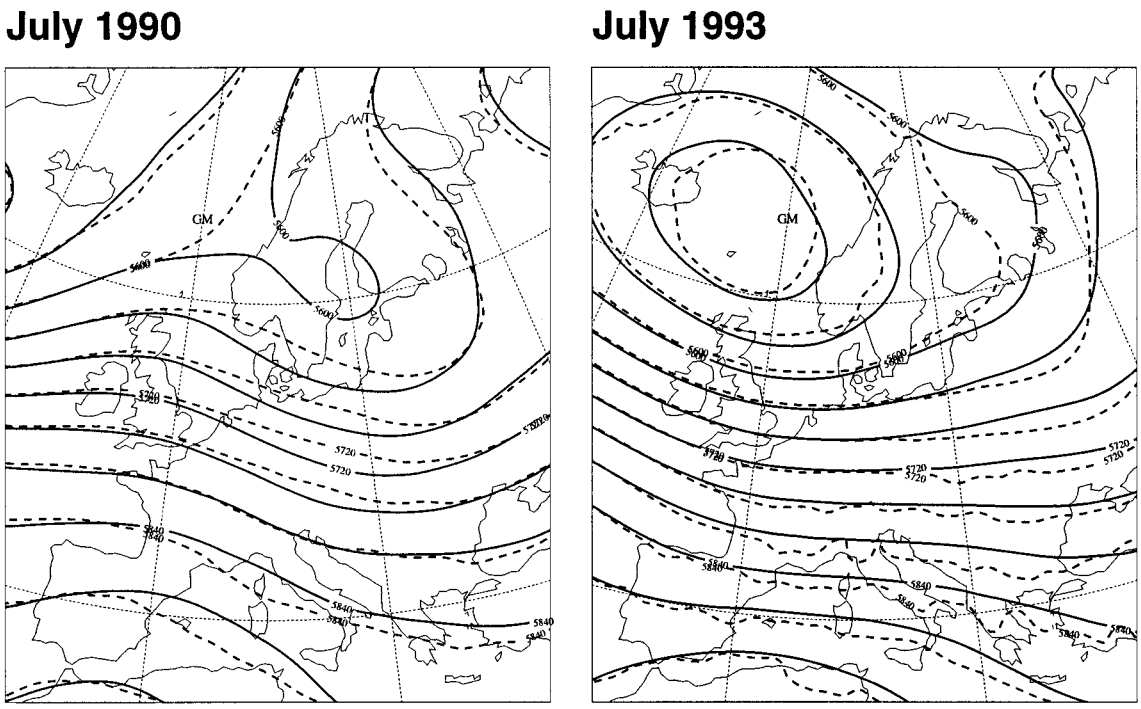

FIG. 3. Monthly mean 500-hPa geopotential for July 1990 (left-hand panel) and July 1993 (right-hand panel) for the control experiments. Shown are the ECMWF analysis (dashed lines) and the simulation (full lines).

back processes, a qualitative initialization of the soil moisture is sufficient.

A certain complication also arises from changes in the operational ECMWF soil moisture assimilation cycle, which has experienced several modifications between 1990 and 1993. We have investigated the alternative to use the ECMWF reanalysis (which uses a homogeneous assimilation scheme since 1979) rather than operational analysis, but the reanalyzed soil moisture fields for 1 July show unrealistically high values close to saturation, even in Mediterranean regions. In contrast, the summertime partial drying of the soil over of central Europe is visible in the NCEP–NCAR reanalysis (Kalnay et al. 1996).

4. Control integration

The control integrations (CTRL) are identical to two simulations already presented in Lüthi et al. (1996) except for the formulation of the evapotranspiration (see section 2). The latter change is comparatively small and primarily affects the hydrological cycle. Thus the discussion of the CTRL runs can be kept brief.

Figure 3 shows the monthly mean 500-hPa geopotential for both the ECMWF analysis (dashed lines) and the simulation (full lines). As discussed in greater detail in Lüthi et al (1996), the simulations capture the analyzed synoptic-scale flow evolution and the generation, progression, and decay of individual low-pressure systems rather well. Analysis of the temporal evolution of the rms difference between the analyzed and simulated 500-hPa height (not shown) demonstrates that the error initially grows up to day ~3 of the integration and subsequently equilibrates at an error level of ~30 gpm. This error level is comparable to that of a typical 2–3-day operational weather forecast. This indicates that the dynamics within the model domain is essentially deterministically controlled by the driving lateral ECMWF boundary fields and that individual low pressure systems transit across the domain in a similar fashion as in the analysis. In essence, a balance is achieved between the transmission of true temporal information of the driving fields into, and the advection of internally generated error out of, the model domain. Furthermore, for the comparatively small computational domain under consideration, the chaotic components of the synoptic-scale dynamics are mostly suppressed. This was further verified by conducting true ensemble integrations, which were identical to the CTRL run except for shifting the initialization time in steps of 24 h. The results (not shown) demonstrate that associated changes in the hydrological cycle were of a small-scale nature and only marginally affect the domain means as considered in the current study.

In Fig. 4 we display the total monthly precipitation for the two control integrations along with an objective analysis of ~1300 rain gauge observations over a part of the domain (for further details see Lüthi et al. 1996). Several features are worth noting. First, the model captures the continental-scale gradient between wet regions

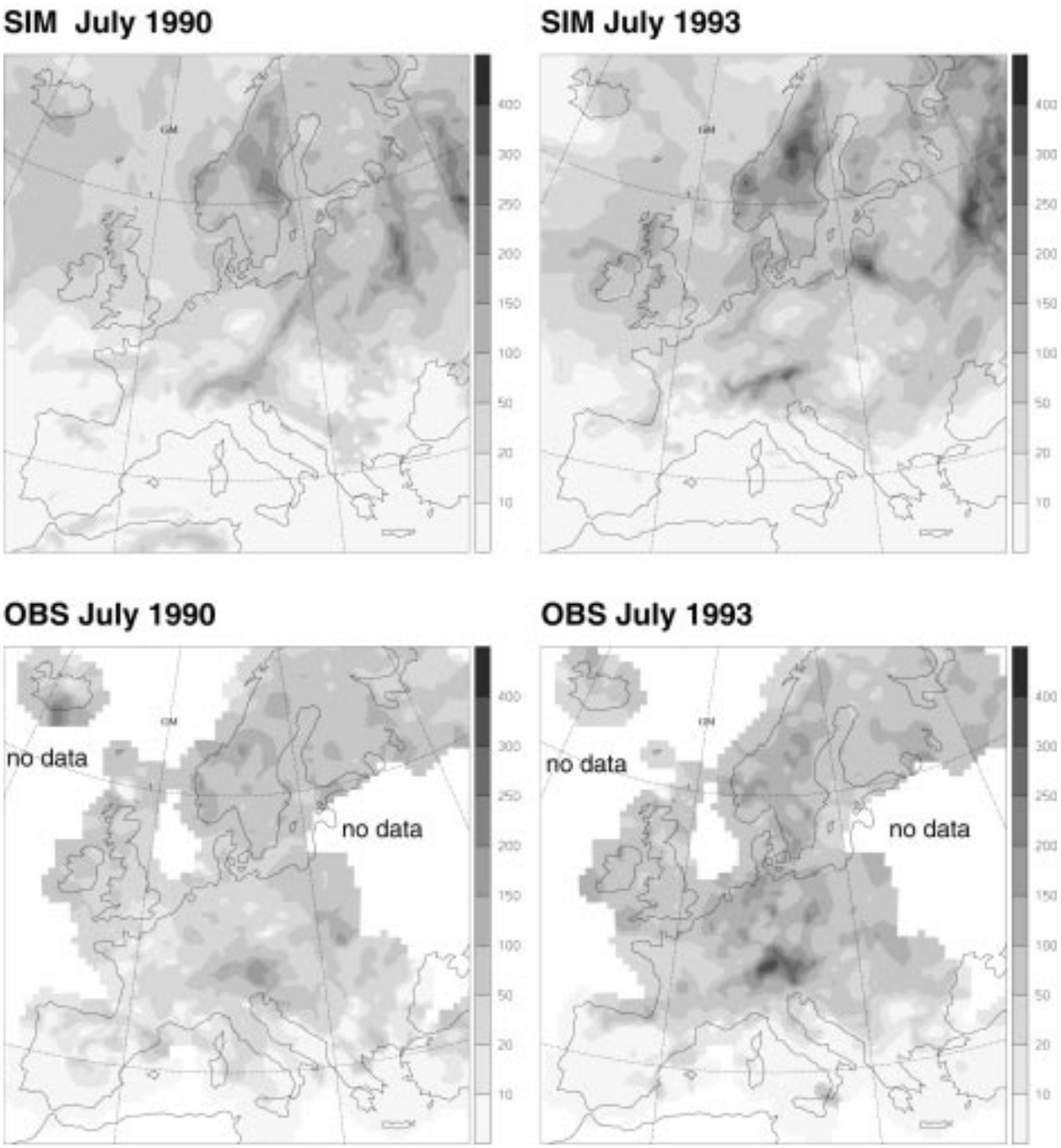

FIG. 4. Monthly precipitation amounts for July 1990 (left-hand panels) and July 1993 (right-hand panels) for the control experiment (CTRL: top panels) and the observations (bottom panels). The validating analysis is only available for a part of the domain.

to the north and dry regions over the Mediterranean. Second, on the subcontinental scale there is some indication that the two simulations capture the characteristic differences between the two years. Note, for instance, that July 1990 was associated with higher values of precipitation in much of France and the Alpine region, in both the observations and the model integrations. However, the difference between the two months is underestimated in the simulations. Third, there are some pronounced simulation errors such as the overestimation of precipitation over Scandinavia and the underestimation over parts of the Mediterranean. These simulation errors primarily derive from inappropriate initial soil moisture conditions and from inaccuracies in the numerical parameterization of moist convection, radiation, and planetary boundary layer processes.

To conclude the analysis, we show for illustration in Fig. 5 the time trace of the mean simulated precipitation over domain FR (France), along with the mean relative water content in the three soil layers over the same area. It can be observed that over this analysis domain most of the precipitation falls in a few episodes. Usually such episodes of summertime precipitation over Europe are associated with the approach of a cyclone toward Great Britain or Scandinavia and the progression of an upper-level trough with its associated low-level cold front toward the continent. This synoptic situation normally leads to convective activity over the continent. This is consistent with the simulated partition of precipitation into large-scale (resolved) and convective (parameterized) contributions: According to our simulation, precipitation over domain FR is to 68% (July 1990) and 78% (July 1993) of convective origin.

Over most of continental Europe, the simulations imply that the atmosphere exports moisture from land to sea. For instance, for the CTRL integration over domain FR, monthly evapotranspiration exceeds precipitation by 48 mm (July 1990) and 23 mm (July 1993), respectively. These values are roughly consistent with the estimates of Alestalo (1983), who used conventional sounding data to compute the divergence of the atmospheric water vapor flux over central Europe.

The bottom panels of Fig. 5 show the reaction of the soil model to the forcing by evapotranspiration and precipitation. Overall there is a drying out of the soil, as is qualitatively consistent with the summer season. Individual precipitation events are associated with a pronounced signal in the uppermost soil layer (with a depth of 2 cm), which slowly migrates and disperses into the lower levels by infiltration and percolation.

5. Sensitivity experiments

Here we compare the CTRL experiment with the sensitivity experiments DRY and WET, which are initialized with modified soil moisture distributions (see section 3 for details) but identical to CTRL in terms of the lateral boundary forcing. We start the discussion of the sensitivity experiments by showing in Fig. 6 the total monthly evapotranspiration and precipitation over selected analysis domains (see Fig. 2 for location of domains). The respective values are given as a function of the soil moisture factor applied to the initial soil moisture field (0.5 for DRY, 1 for CTRL, 2 for WET). Qualitatively, the results are similar for the two months. Over the land domains SP, FR, and CE both evapotranspiration and precipitation increase with increasing initial soil moisture. For instance, over domain FR for the month of July 1990, evapotranspiration increases from 9 mm/month (in experiment DRY) over 67 mm/month (CTRL) to 99 mm/month (WET), while precipitation increases at a comparable rate from 10 mm/month (DRY) over 20 mm/month (CTRL) to 33 mm/month (WET). For this region, the changes in precipitation amount to a noteworthy fraction of those in evapotranspiration, namely to 42% for WET − CTRL, and to 17% for CTRL − DRY. In contrast and as to be expected, soil-moisture-induced changes over the oceanic areas AT (Atlantic) and MS (Mediterranean Sea) are small.

Although the soil has a notable effect in most of the domain, the relative changes in precipitation, here defined as (WET − DRY)/CTRL, show a specific geographical distribution (see Fig. 7). For both the sensitivity ensembles, relative changes are particularly large in a band that extends from Spain over France into central and southern Europe. In this band, the soil–precipitation feedback is most effective. The results thus indicate that the boundary between the wet Atlantic climate and the dry Mediterranean climate heavily depends upon the soil moisture distribution.

Figure 8 shows the simulated evolution of the mean total soil moisture content over the analysis domain FR. Each of the panels shows the results for one month and all the three experiments. All the integrations are characterized by a drying out of the soil. In the experiments DRY and WET, the soil moisture content shows a tendency to relax toward the CTRL integration. Assuming that the initial soil moisture anomalies decay exponentially with $e^{-\sigma t}$, we find for the timescale σ^{-1} values between 1.7 and 3.9 months. These values serve to characterize the long-term memory associated with soil moisture anomalies.

The strong sensitivity of the precipitation response with respect to the soil moisture content that is seen in the current study is in qualitative agreement with the results of Rowntree and Bolton (1983). In their study, Rowntree and Bolton used a low-resolution GCM and conducted a systematic set of experiments in which they compared the GCM's response to initial dry and wet soil moisture anomalies. The high-resolution computations presented here confirm their results but give a more detailed account of the regional distribution of the sensitivity and of the underlying physical processes.

6. Budget analysis

In this section we conduct a budget analysis to analyze the atmospheric fluxes of water and to test the two hypothesis earlier alluded to in Fig. 1. To this end we will use two bulk characteristics to describe the regional water cycle over selected subdomains. The characteristics considered are the recycling rate β and the precipitation efficiency χ. Both of these characteristics will be defined for selected subdomains. Following Budyko (1974) and Brubacker et al. (1993), the recycling rate β is defined as the fraction of precipitation in a certain analysis domain that originates from evapotranspiration from within the same domain. Similarly, the precipitation efficiency χ describes the fraction of water that enters the domain (either by evapotranspiration or atmospheric transport) and subsequently falls as precipitation within it. These two quantities are regarded

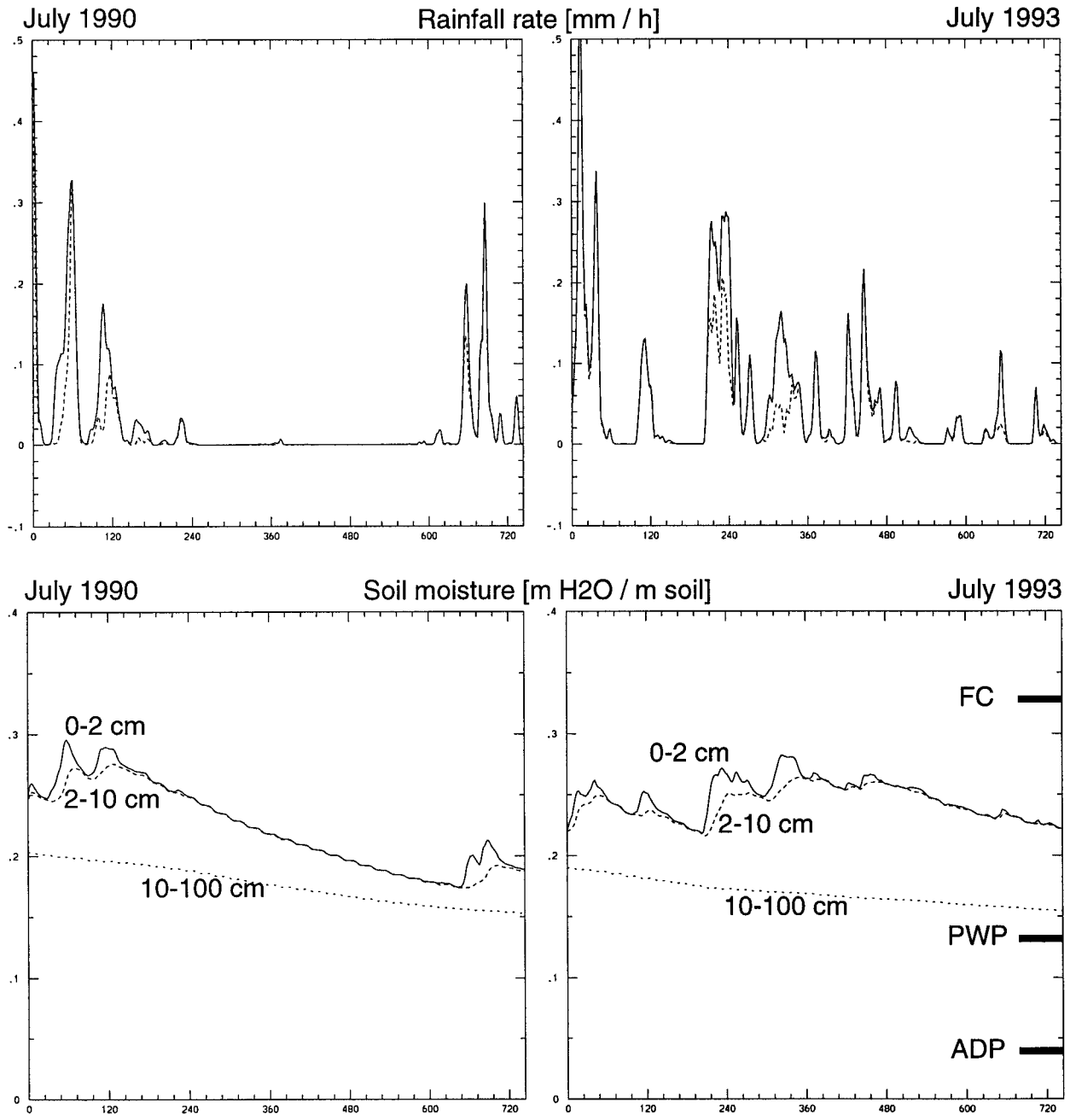

FIG. 5. Simulated precipitation rate (top panels) showing total precipitation (full line) and convective contribution (dashed line). The bottom panels show the evolution of soil moisture (m H_2O/m soil) in the three soil layers. The data is for experiment CTRL and the analysis domain FR (see Fig. 2), for July 1990 (left-hand panels), and July 1993 (right-hand panels). Labels in bottom panels relate to the mean values of the air-dryness point (ADP), the field capacity (FC), and the plant wilting point (PWP) over the analysis domain FR.

as bulk properties of the regional water cycle, and their determination from model output data is described in the next subsection.

a. Theory and methodology

For the budget analysis we define boxes that are confined below by the earth's surface and laterally by vertical walls. The location of the boxes is shown in Fig. 2. Two of the boxes are located over the Atlantic Ocean and Mediterranean Sea, respectively, while the other three boxes are over land. For each of the boxes the relevant monthly mean water fluxes IN (flux into the domain), OUT (flux out of the domain), ET (evapotranspiration), and *P* (precipitation) shown in Fig. 9 are diagnosed form the model output. We will also allow

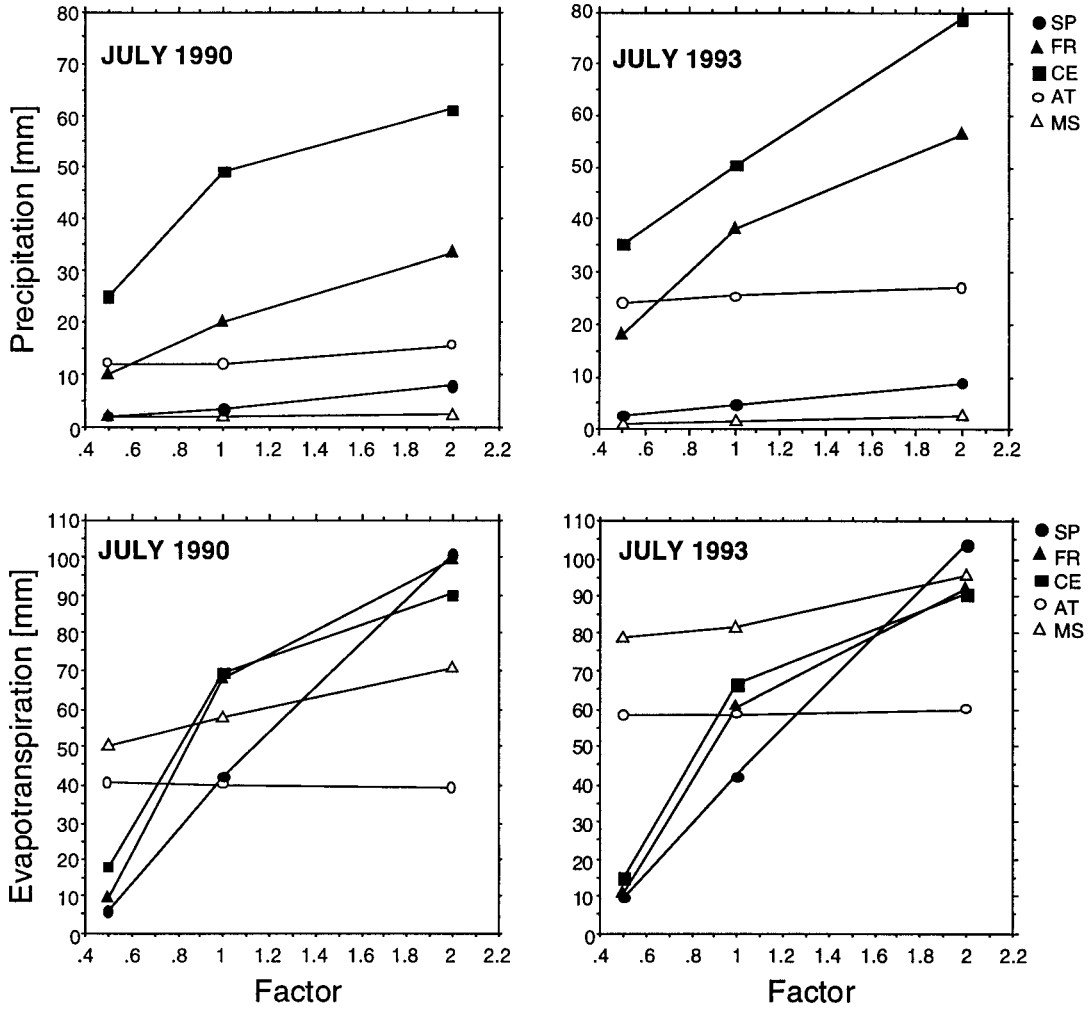

FIG. 6. Simulated total precipitation (top panels) and evapotranspiration (bottom panels) in mm/month for July 1990 (left-hand panels) and July 1993 (right-hand panels) as a function of the factor applied to the initial soil moisture content. The various curves relate to the analysis domains shown in Fig. 2.

for a change of the total atmospheric water content W within the box, but this term is small, has a negligible impact upon the results, and is only considered for internal consistency. The associated budget relationship for each box can then be written as

$$\Delta W = \text{IN} - \text{OUT} + \text{ET} - P. \quad (1)$$

Here all the flux terms are integrated over the time period under consideration (selected as one month), and ΔW denotes the integrated tendency of the atmospheric water content within the box.

For the computation of the recycling rate we assume, following the pioneering work of Budyko (1974), that the two water fractions that originate from evapotranspiration within and outside of the box, respectively, are well mixed—both in space and time. As discussed by Budyko, this implies that the recycling rate β directly denotes the fraction of moisture that originates from evapotranspiration within the box and is identical for all types of water substance (i.e., water vapor, cloud water, and precipitation).

Assuming a constant recycling rate within each box allows one to easily determine β from the associated water fluxes. Individual budget relations similar to (1) may be expressed for the two fractions of water that derive from evapotranspiration in the interior of the domain and from atmospheric advection into the domain, respectively. For instance, for the budget of water that originates from within the box, the term IN disappears, while the terms OUT, P, and ΔW appear with a factor β, consistent with the assumption of a uniform recycling rate. The two budgets are then given by

$$\Delta W\beta = -\text{OUT}\beta + \text{ET} - \text{P}\beta$$
$$\Delta W(1 - \beta) = \text{IN} - \text{OUT}(1 - \beta) - \text{P}(1 - \beta). \quad (2)$$

Solving for β and substituting from (1) yields

$$\beta = \text{ET}/(\text{IN} + \text{ET}). \quad (3)$$

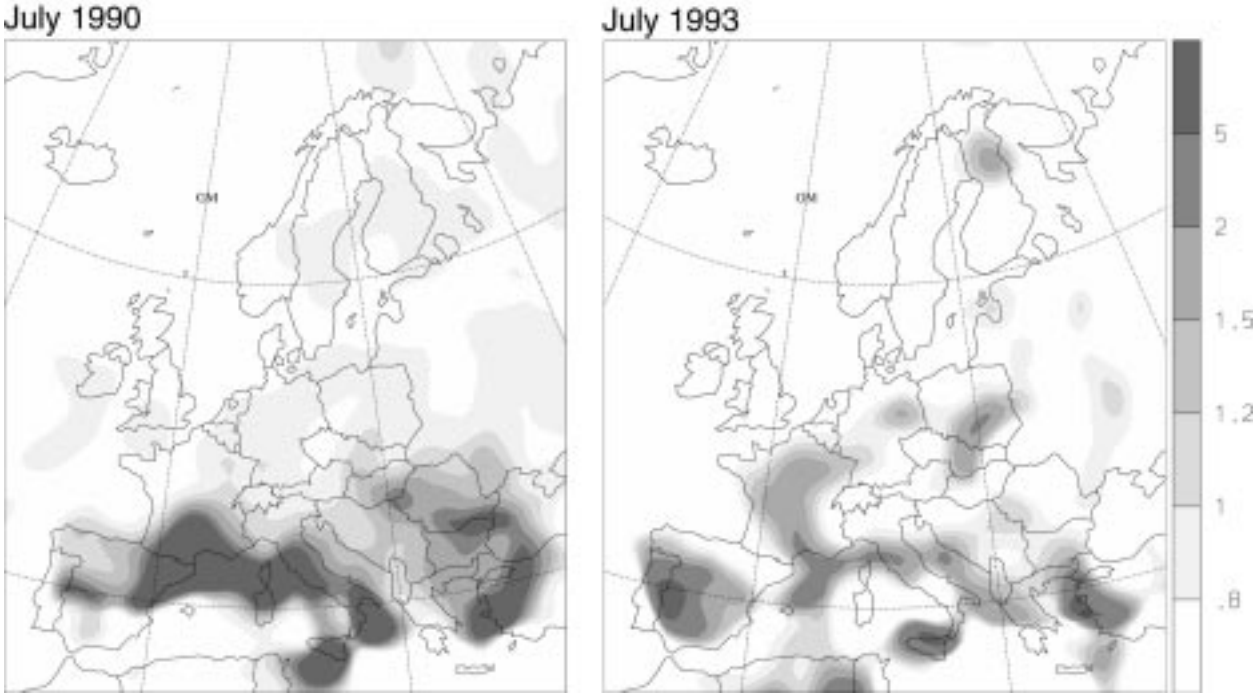

FIG. 7. Smoothed geographical distribution of the monthly mean normalized precipitation sensitivity computed as (WET − DRY)/CTRL.

Similarly, the precipitation efficiency χ can directly be computed from its definition as

$$P = \chi(\mathrm{IN} + \mathrm{ET}). \quad (4)$$

According to this relationship, χ describes the fraction of water that enters the box (either through evapotranspiration or atmospheric transport) and subsequently falls as precipitation.

As discussed above, Budyko's model is based on the assumption that the water molecules that derive from within and outside the analysis box are well mixed. This assumption is well justified in the vertical direction,

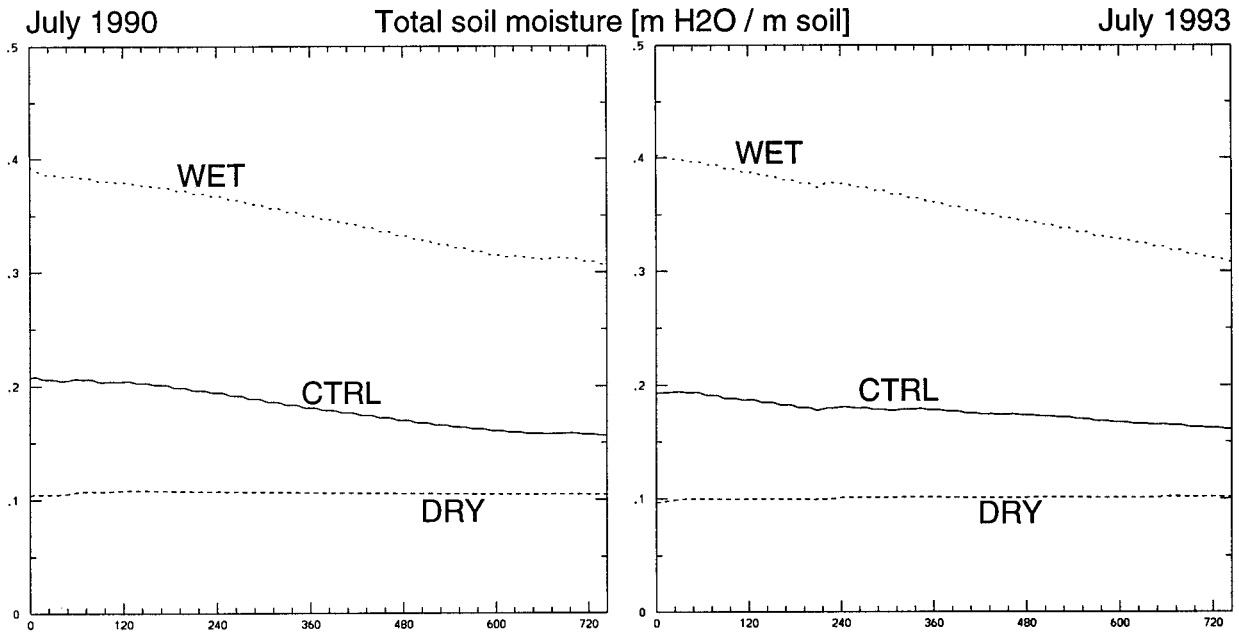

FIG. 8. Simulated evolution of mean total soil moisture content over the analysis domain FR (m H_2O/m soil) for the experiments DRY, WET, and CTRL.

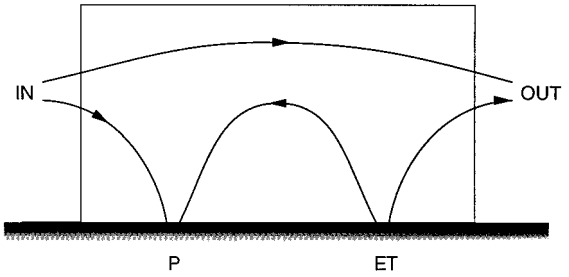

FIG. 9. Definition of water fluxes in analysis domains: inflow (IN), outflow (OUT), evapotranspiration (ET), and precipitation *P*.

where boundary layer turbulence and convective processes lead to rapid mixing over timescales comparable to the advective timescales—particularly during summertime conditions as considered in our study. In the horizontal direction, however, the assumption is not so well justified since horizontal variations in temperature and relative humidity across the boxes can be substantial. Several studies have addressed this limitation, among them those of Burde et al. (1996) and Eltahir and Bras (1994). The latter authors conducted an intercomparison over the Amazon region with a three-dimensional version of Budyko's model, allowing for horizontally varying recycling rates. Their results indicated that the errors associated with assuming a horizontally well-mixed distribution of water fractions is of quantitative rather than qualitative nature. An alternative way to estimate the recycling rate was pioneered by Joussaume et al. (1984). In order to estimate the origin of precipitating water, they used a GCM and tagged water evaporating from various source regions. This methodology was used in a range of subsequent studies (e.g., see Koster et al. 1986; Jouzel et al. 1997) and generally yielded higher values of the recycling rate than anticipated from earlier work.

Despite some uncertainties about the range of validity of Budyko's assumptions, his model will here be applied in some qualitative sense. For most of our study β and χ as defined by (3) and (4) can be regarded as bulk properties of the regional water cycle within some analysis domain. In this sense, these measures are not directly linked to Budyko's assumptions but nevertheless summarize useful information about the relative magnitude of the relevant water fluxes.

For the computation of β and χ as outlined above, the relevant water fluxes for each of the boxes shown in Fig. 2 were diagnosed from the model output. Since the atmospheric fluxes IN and OUT contain eddy contributions, they must be averaged over the month-long integration from the wind, water vapor, and liquid water content. The adopted averaging is based on 12-h output data. Comparison of results obtained with shorter averaging periods (down to 1 h) confirmed that an output interval of 12 h is sufficient for the current purpose. Nevertheless, the procedure entails some small errors, which imply that the budget relation (1) is only approximately satisfied. For internal consistency, we have thus corrected the atmospheric fluxes IN and OUT such as to fully satisfy the budget constraint (1). To this end, the imbalance

$$\varepsilon = \mathrm{ET} - P + \mathrm{IN} - \mathrm{OUT} - \Delta W \qquad (5)$$

is computed for each box, and subsequently distributed equally over the atmospheric fluxes according to

$$\mathrm{OUT}^{\mathrm{corr}} = \mathrm{OUT} + \varepsilon/2 \quad \text{and} \quad \mathrm{IN}^{\mathrm{corr}} = \mathrm{IN} - \varepsilon/2. \qquad (6)$$

The corrected fluxes then fully satisfy the budget constraint. The associated corrections are small and are only introduced for internal consistency. Recycling rates and precipitation efficiencies computed from the uncorrected fluxes IN and OUT were, in all cases, very similar to the those computed from $\mathrm{IN}^{\mathrm{corr}}$ and $\mathrm{OUT}^{\mathrm{corr}}$.

b. Results and discussion

Figure 10 shows the results in terms of the recycling rate β and the precipitation efficiency χ for each of the boxes considered. The results are again displayed as a function of the initially applied soil water factor. Both bulk characteristics show a pronounced dependence upon the initial soil moisture content over the land domains. For instance, over domain FR in July 1990, the precipitation efficiency increases from 1.6% for DRY to 4.4% in experiment WET. Changes of similar magnitude are also evident in the recycling rate. In contrast, over the sea domains AT and MS, the changes are much smaller and are presumably associated with episodes of flow from land to sea.

The diagnosed increases of the bulk precipitation efficiency and recycling rate with increasing soil moisture imply that the nature of the precipitation processes are highly sensitive to the soil moisture content. In fact, the observed increase of precipitation cannot be interpreted by the classical recycling mechanism. Consider for illustration the changes between experiment CTRL and WET over domain FR for the month of July 1990 (see also Fig. 6). Here evapotranspiration increased by 31 mm/month, and precipitation by a comparable amount of 14 mm/month. To explain the observed behavior by simple precipitation recycling would require returning a large fraction (almost 50%) of the increase in evapotranspiration in the form of precipitation over the same domain. However, this interpretation is not justified in view of the diagnosed precipitation efficiencies of between 1.6% and 4.4%. Thus, the ''recycling hypothesis'' alluded to in Fig. 1 must be rejected.

For a more quantitative analysis, we now consider the changes in precipitation by further analysis of Eq. (4). To this end, let

$$P = \chi(\mathrm{IN} + \mathrm{ET}) \qquad (7a)$$

express the conditions in the CTRL experiment over any of the analysis domains. A similar relationship also

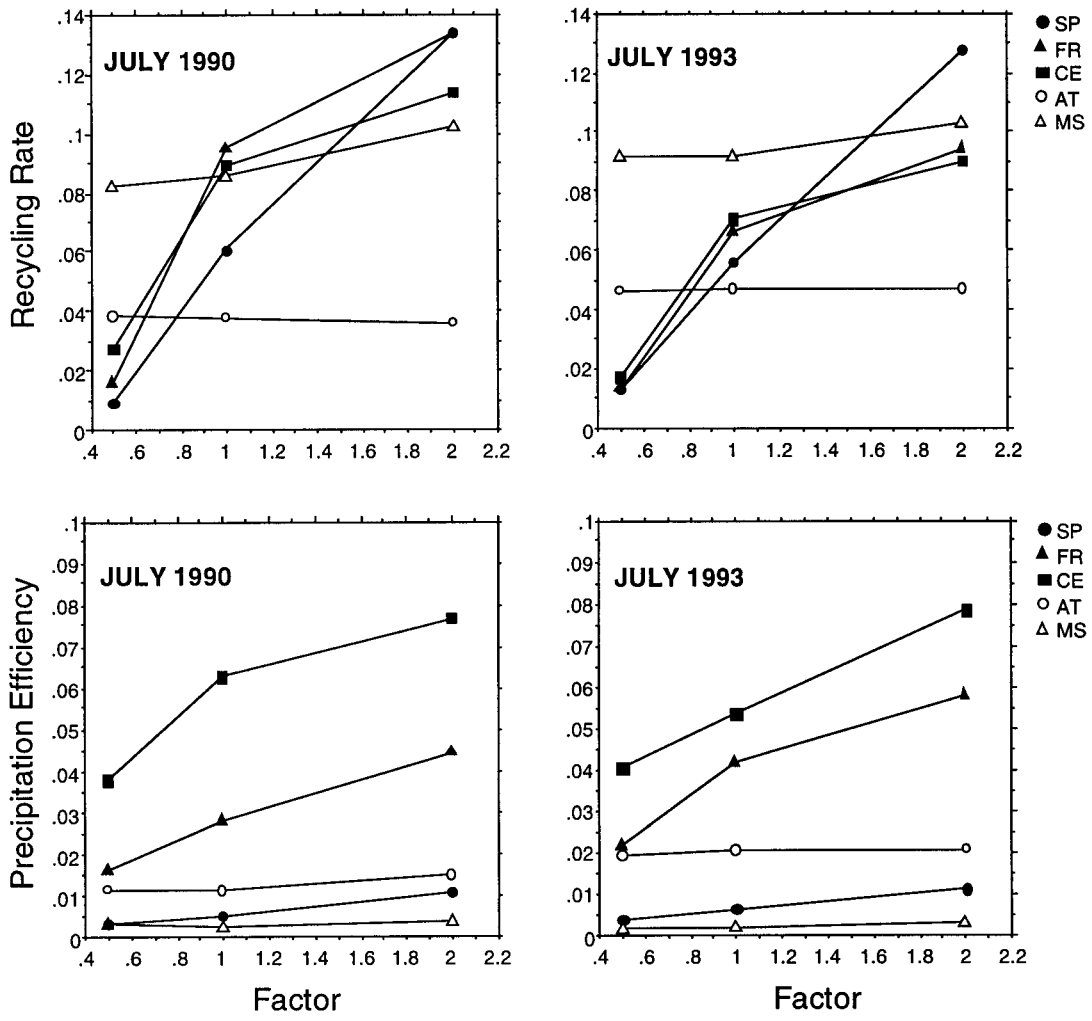

FIG. 10. Recycling rate β (top panels) and precipitation efficiency χ (bottom panels) for all analysis domains as a function of the initial soil moisture factor for July 1990 (left-hand panels) and July 1993 (right-hand panels).

holds for either one of the two sensitivity experiments, that is,

$$P' = \chi'(\mathrm{IN}' + \mathrm{ET}'), \tag{7b}$$

where dashed variables denote the conditions in the sensitivity experiment. The aim of the subsequent analysis is to attribute changes in precipitation, that is,

$$\Delta P = P' - P, \tag{8}$$

to either one of the two hypothesis earlier alluded to in Fig. 1. Substitution from (7) yields

$$\Delta P = \chi'(\mathrm{ET}' + \mathrm{IN}') + \chi(\mathrm{ET} + \mathrm{IN}),$$

and careful rearrangement of the terms allows one to express ΔP as

$$\Delta P = \chi'(\Delta\mathrm{ET} + \Delta\mathrm{IN}) + \Delta\chi(\mathrm{ET} + \mathrm{IN}). \tag{9}$$

The first term of this equation isolates those contributions associated with changes in the water fluxes ΔET and ΔIN, while operating with a constant precipitation efficiency χ'. It thus essentially corresponds to the recycling hypothesis alluded to in Fig. 1a. In contrast, the second term isolates those contributions associated with changes in the precipitation efficiency $\Delta\chi = \chi' - \chi$. This term does not explicitly depend upon changes in the evapotranspiration and corresponds to the indirect hypothesis alluded to in Fig. 1b.

Using the diagnosed values from our simulations, the contribution of the two terms to the simulated precipitation changes can objectively be assessed. The results are shown in Fig. 11 in the form of bar diagrams. For each simulation and domain, the two bars correspond to the changes DRY − CTRL and WET − CTRL, respectively. During both months and in all the analysis domains, the changes are clearly dominated by the second term in (9). This implies that the simulated sensitivity cannot be explained by the recycling concept since the return of evaporated water as precipitation (the hatched portion of the bars) can account for only around 10% of the simulated changes (the full length of the

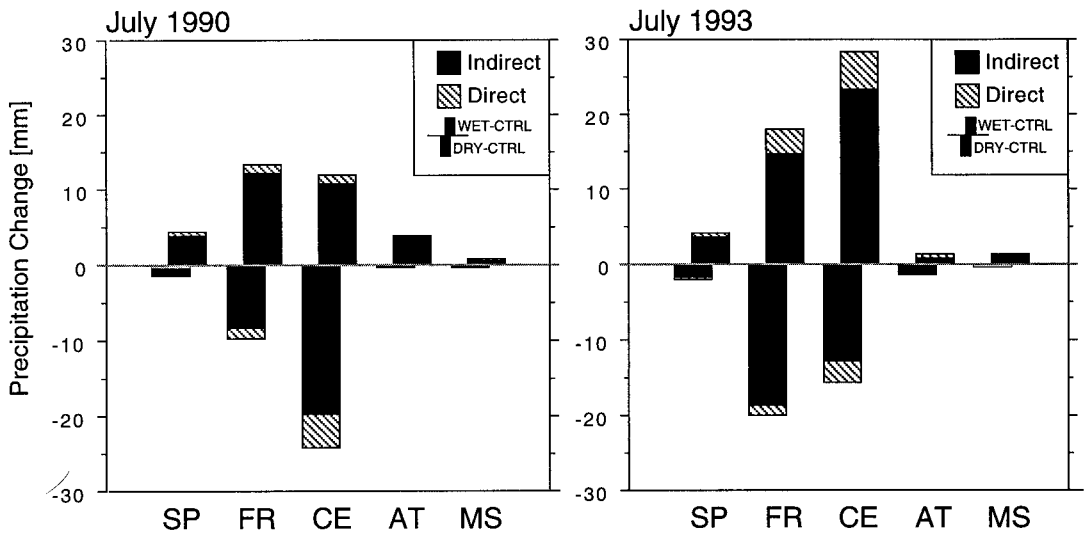

FIG. 11. Changes in precipitation for DRY − CTRL (downward-looking bars) and WET − CTRL (upward-looking bars) in mm/month. Each pair of bars relates to one specific analysis domain (see Fig. 2). The shading of the bars relates to the contribution of the two terms in (9). Hatched portions of the bars relate to the left-hand term in (9) associated with the direct (recycling) hypothesis, while black portions of the bars relate to the right-hand term associated with the indirect (precipitation efficiency) hypothesis.

bars). In contrast, the analysis implies that the main factor responsible for the sensitivity is related to changes in precipitation efficiency (the black portion of the bars).

The importance of the second term in (9) should not be too surprising, given the magnitude of the terms involved. For the domains considered, the IN and OUT terms are by far the largest (e.g., for July 1990, domain FR and experiment CTRL: IN = 616 mm/month compared to ET = 44 mm/month). Since changes in precipitation efficiency act directly upon the water fluxes entering the domain, comparatively small changes in precipitation efficiency can thus explain substantial changes in precipitation.

7. Process analysis

In this section we analyze the physical processes that are responsible for the simulated soil–precipitation feedback. To this end, attention is restricted to July 1990 and domain FR, which approximately covers France. Results for other analysis domains over continental Europe are qualitatively very similar.

a. Diurnal cycle of surface variables

We begin by discussing the mean diurnal cycle of evapotranspiration and precipitation over the analysis domain FR in the month of July 1990. The evapotranspiration rates for experiments DRY, CTRL, and WET (see Fig. 12a) reflect the strong sensitivity of the surface moisture fluxes shown earlier in Fig. 6. Evapotranspiration is almost shut off in the DRY experiment, while in the WET experiment noon peak values reach 0.35 mm h^{-1}. These large differences are consistent with the soil moisture content (see Fig. 8), which is below the turgor loss point in the DRY experiment (near saturation during most of the WET experiment). The large variations in evapotranspiration between the experiments imply major differences in the Bowen ratio (which measures the ratio between sensible and latent heat flux). The corresponding mean-monthly values for the three experiments DRY, CTRL, and WET are 9.7, 0.93, and 0.44, respectively.

Figure 12b shows the mean diurnal cycle of precipitation averaged over domain FR. Depending on the simulation, two precipitation peaks are represented with different amplitudes. Precipitation in the CTRL experiment reaches maximum in the early afternoon (peak value around 1300 local time). In the DRY experiment the early afternoon precipitation peak is essentially removed, and mean maximum precipitation intensity is in the early morning. In the WET experiment, a typical convective precipitation cycle is evident with a pronounced afternoon and a weaker, but still well-defined, early morning precipitation peak. This type of diurnal precipitation cycle is well documented for summertime central European conditions, albeit the timing of the afternoon precipitation peak is too early (caused by a too rapid temperature increase in the early morning). The late afternoon peak is usually interpreted as a direct result of the diurnal cycle of shortwave heating at the earth's surface, while the early morning peak results from longwave nighttime radiative cooling at cloud-top levels, two processes which tend to shift the vertical stratification toward a convectively unstable profile. The characteristic diurnal precipitation peaks in Fig. 12b

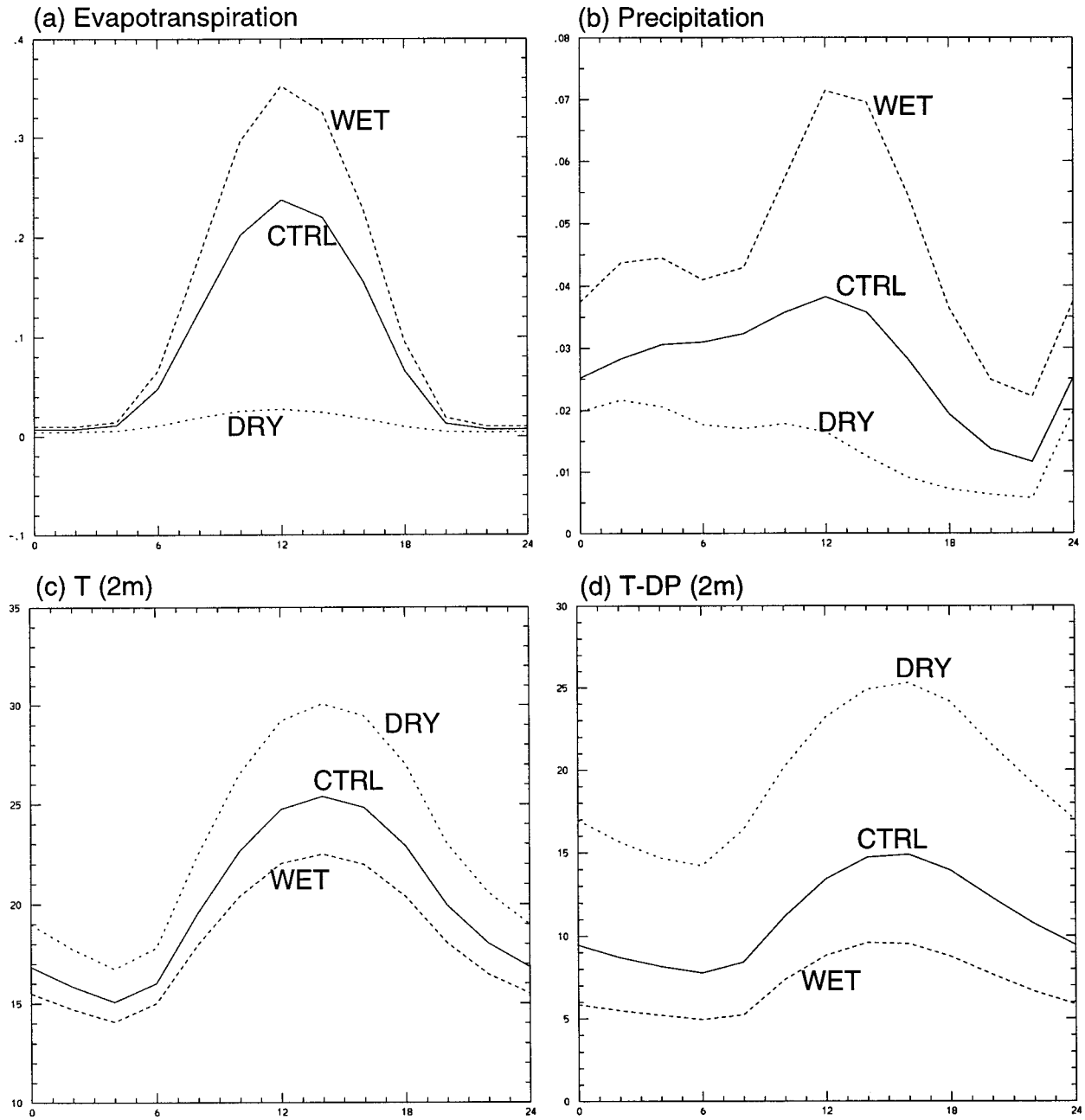

FIG. 12. Mean diurnal cycle over domain FR and for July 1990. Panels (a) and (b) show evapotranspiration and precipitation in mm h^{-1}, panels (c) and (d) the 2-m temperature and dewpoint difference in °C. The three curves relate to the three experiments DRY, CTRL, and WET.

thus imply that the simulated precipitation differences between experiments DRY, CTRL, and WET must primarily result from summertime convective activity. This is consistent with the model results, which show that differences in precipitation are dominated by subgrid-scale convection.

To complete the analysis, Figs. 12c,d show the diurnal cycle of 2-m temperature and dewpoint difference. Both are substantially higher over dry soil. This aspect is consistent with the increased fraction of energy that is carried away from the surface by sensible rather than latent heat fluxes.

b. The development of the daytime well-mixed boundary layer

Since the soil–precipitation feedback process relies on convective activity and is characterized by a strong diurnal cycle, the analysis of the underlying mechanism must seek to explain the development of convective

instability during the buildup of the well-mixed boundary layer in response to solar heating. For analysis, Fig. 13 depicts the evolution of the daytime boundary layer over domain FR in terms of potential temperature, relative humidity, and the pseudopotential temperature θ_e, both for the DRY (left-hand panels) and WET (right-hand panels) experiments. These profiles represent the monthly mean diurnal cycle averaged over a large area of 900×800 km^2. This area is represented in the model by approximately 230 grid points.

After sunrise (at around 0500 UTC), the net surface radiation balance becomes positive and the associated energy is transmitted into the boundary layer. The structure and depth of the growing boundary layer is then primarily determined by the Bowen ratio, that is, the ratio between sensible and latent heat fluxes at the earth's surface. In the dry case, the Bowen ratio is large and the net radiative energy balance at the surface is converted into sensible heating, resulting in the buildup of a deep well-mixed boundary layer. This process is well captured by the θ panels in Fig. 13. The depth of the well-mixed boundary layer corresponds to about $\Delta p \sim 150$ hPa in experiment DRY, while in the WET case sensible heating is much smaller, and the resulting boundary layer is comparatively shallow ($\Delta p \sim 100$ hPa). Likewise, the input of water vapor into the boundary layer is larger than in the DRY case. Thus, more moisture is distributed over a thinner and cooler boundary in the WET experiment. The combined effect of these two factors is a boundary layer characterized by high relative humidity values. At 1800 UTC they reach ~70% in WET compared to ~30% in DRY (see Fig. 13, middle panels).

It is important to realize that the aforementioned differences in relative humidity do not reflect differences in specific humidity. In fact, the mean monthly water content (computed from 6-h data) over the domain under consideration amounts to 19.76, 20.89, and 21.95 mm for the simulations DRY, CTRL, and WET, respectively. The surprisingly small differences between these values confirm that the primary distinction between the simulations is not related to the water content itself, but rather to the near-surface temperature profiles, which ultimately control the relative humidity and the degree of instability. The small differences in specific humidity also emphasize that most of the water content in the domain does not derive from local sources but is rather advected into the domain from outside. According to the estimation of the recycling rate (see Fig. 10), the local contribution of evapotranspiration from within the box to the total water content amounts to 1.6%, 9.4%, and 13.2%, respectively, for the three simulations. While these values might somewhat underestimate the real contribution as a result of the idealized assumptions inherent to the Budyko recycling model (see the discussion in section 6a), their order of magnitude is consistent with the overall changes in mean water content and mean evapotranspiration, both of which have changed by the same order of magnitude.

The lowermost panels in Fig. 13 show the evolution of the pseudopotential temperature θ_e. This profile can be viewed as the most important aspect of the thermodynamic stratification since it is directly related to convective instability. In the WET experiment there is a well-defined boundary layer of elevated θ_e values. In contrast, in experiment DRY, the low-level distribution of θ_e is very flat. The differences between the two evening profiles are very pronounced. Experiment WET is—in terms of pseudopotential temperature—warmer at low levels but colder aloft. Both these differences contribute to the higher potential for convective instability in the WET simulation. The release of this instability is facilitated by lowering the level of free convection, which is promoted by the moistening of the boundary layer discussed above.

It is important to note that the strikingly different structures evident in the θ_e profiles do not directly result from the difference in the Bowen ratios. In fact, supplying a certain amount of energy to a volume of air does increase the air parcel's moist entropy by the same amount, irrespective of whether the energy is supplied in the form of latent or sensible heat. Thus the differences between the two θ_e profiles is not a direct response to the different Bowen ratios but rather due to an indirect effect associated with the development of the boundary layer's vertical structure: In the WET experiment (DRY experiment), the moist entropy flux into the boundary layer is concentrated into a thin boundary layer (distributed through a deep layer), as illustrated by the potential temperature structures in the top panels of Fig. 13. The simulated evolution of the planetary boundary layer is thus in accord with the reasoning of Betts and Ball (1995) and Betts et al. (1996), who suggested that the depth of the developing boundary layer is the key factor that governs the soil–precipitation feedback.

The above arguments are also consistent with adopting low-level moist entropy or pseudopotential temperature as a single one-parameter indicator for assessing convective precipitation. Williams and Renno (1993) were able to show, using data from the Tropics, that convective available potential energy is linearly correlated to boundary layer moist entropy, and the realism of such a relationship is also supported by other obser-

→

FIG. 13. Mean diurnal evolution of vertical profile of potential temperature, relative humidity, and pseudopotential temperature θ_e. Results are shown for experiments DRY (left-hand panels) and WET (right-hand panels), and for times 0600, 1200, and 1800 UTC (0700, 1300, and 1900 local time). The profiles start at the first full model level (30 m above ground).

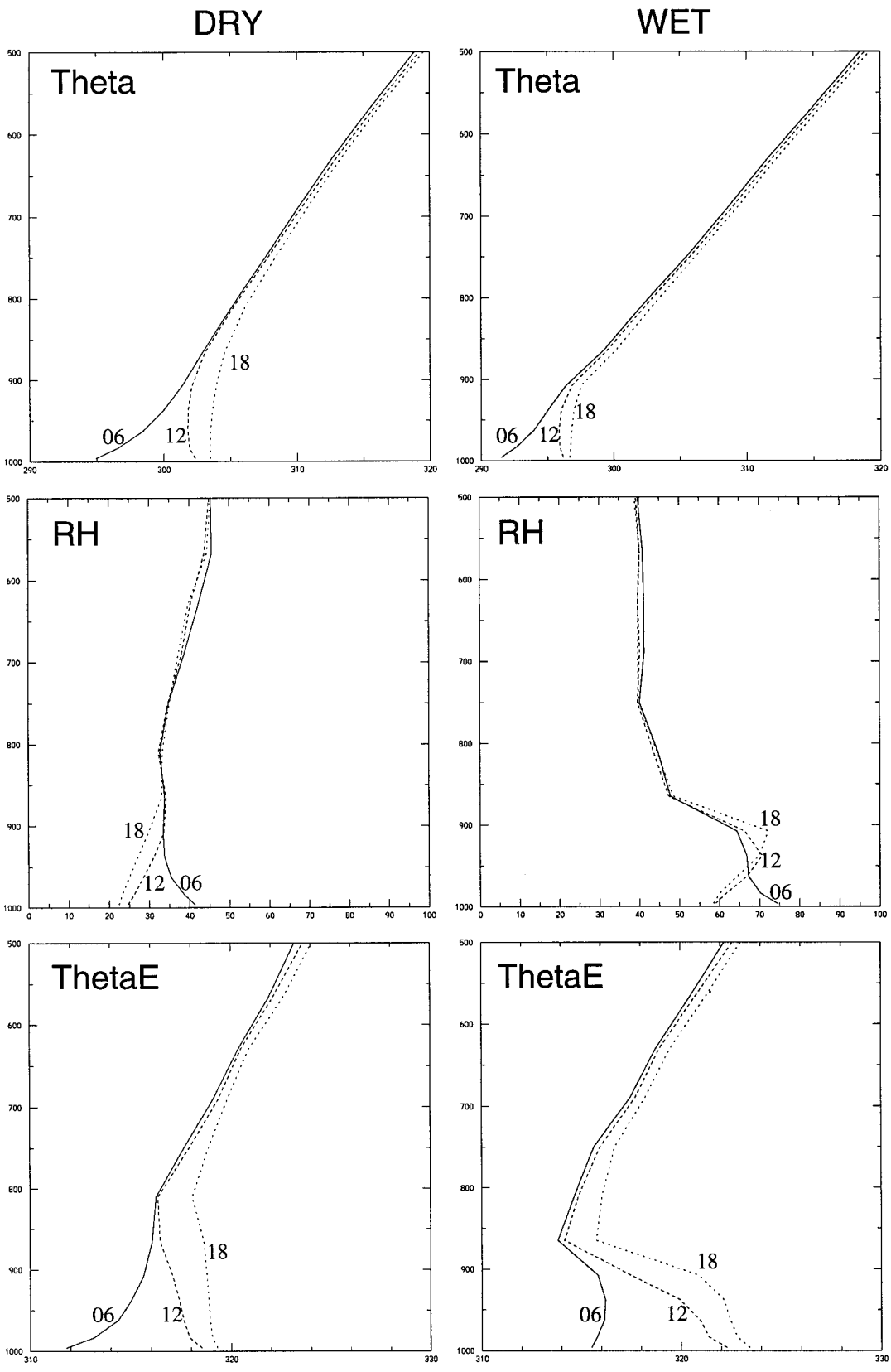
DRY
WET
Theta
Theta
RH
RH
ThetaE
ThetaE
06
12
18

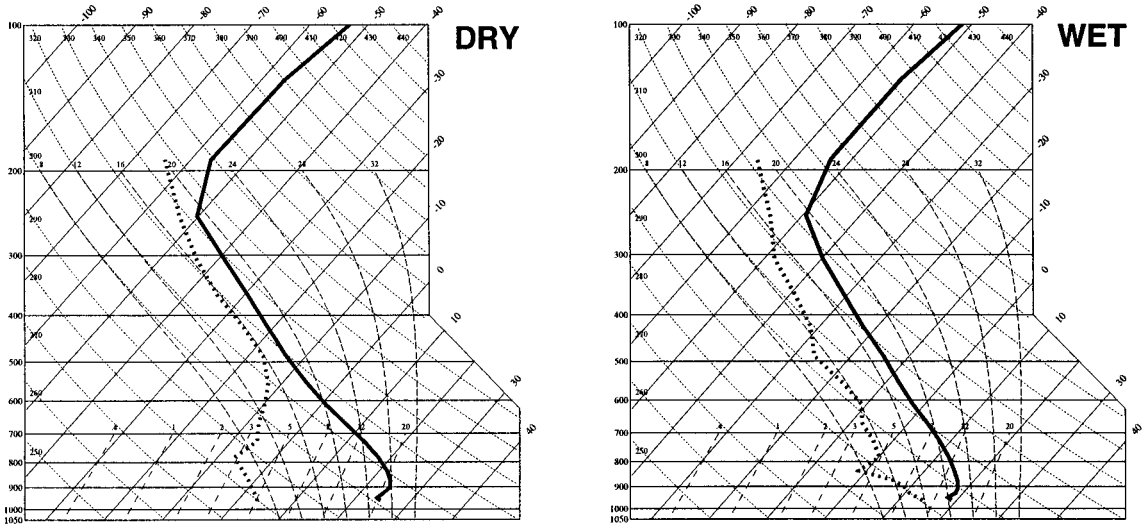

FIG. 14. Tephigram showing temperature and dewpoint averaged over domain FR for DRY (left) and WET (right) at 0800 26 July 1990.

vational data and some theoretical concepts (Eltahir and Pal 1996).

It should be emphasized that the profiles in Fig. 13 pertain to the *area mean* over domain FR and to the *mean diurnal cycle* averaged over the whole month of July 1990. In this mean, convective instability is not reached (the level of free convection is too elevated). However, during specific synoptic episodes conducive to convective activity, the differences inherent to the mean monthly profile may well suffice to promote a transition from convectively stable to unstable conditions. For illustration, Fig. 14 shows domain-mean (domain FR as above) tephigrams for one particular instant, namely 0800 UTC July 26 1990 (time $t = 608$ h of the integration). At this point in time, an upper-level trough approached the continent and lead to a destabilization of the tropospheric profile. Convective instability is reached in the WET integration with a CAPE value of 966 J kg^{-1}, while in the DRY integration the CAPE value is as low as 240 J kg^{-1}. To adiabatically raise a surface air parcel to the level of free convection would require a surface temperature of 32.5°C (experiment WET) and 40°C (experiment DRY). The former CAPE value for simulation WET compares well with those obtained from typical central European soundings on days with widespread moderate to strong convection. On the other hand, high surface temperatures around 40°C—as required in simulation DRY for the initiation of convection—are very rarely observed in Europe and indicate the absence of convection or at best the sporadic occurrence of isolated thunderstorms with elevated cloud base. The analysis thus confirms how the aforementioned processes may act to determine the convective activity on days with suitable synoptic conditions.

c. Radiative feedbacks

The discussion in the above subsection explains how a lower Bowen ratio in conjunction with some given net surface energy balance leads to a higher potential for convective activity. However, one suspects immediately that increased cloud formation could reduce the amount of solar radiation at the surface and thereby provide a negative feedback to the whole feedback loop. For further analysis, we consider in Fig. 15 the mean diurnal cycle of the components of the surface energy balance. The main effect of the soil is clearly evident in terms of the sensible (SH) and latent (LH) heat fluxes. In the DRY simulation, the latent heat flux is almost negligible, while in the WET experiment it exceeds the sensible contribution. In addition, it can also be observed that the shortwave (SW) absorption of solar irradiance is substantially reduced in WET, as to be expected in response to the increased cloud cover. In response, however, there is also a strong effect upon the longwave (LW) radiative component. Although the differences in net longwave emission are comparatively small in amplitude, they persist throughout the day and add up to the dominant contribution.

For more detailed analysis, Fig. 16 shows the mean diurnal cycle of the absorbed SW and LW contributions for the difference WET − DRY. The increase of cloud cover in WET results in a mean reduction of solar input by ~50 W m^{-2} at noon. Likewise, changes in the longwave radiation budget reach a maximum amplitude of similar magnitude but opposite sign in the early afternoon hours. These later changes result from three factors, namely (i) increased longwave cloud backscatter, (ii) increased H_2O greenhouse effect, and (iii) decreased longwave emissions as a result of the reduced soil temperature.

The daily means of these changes amount to −17.4 and +34.5 W m^{-2} for the shortwave and longwave components, respectively. Thus, the reduction in longwave emission is the dominant factor, and the net effect of the radiative feedbacks is rather unexpected: Although

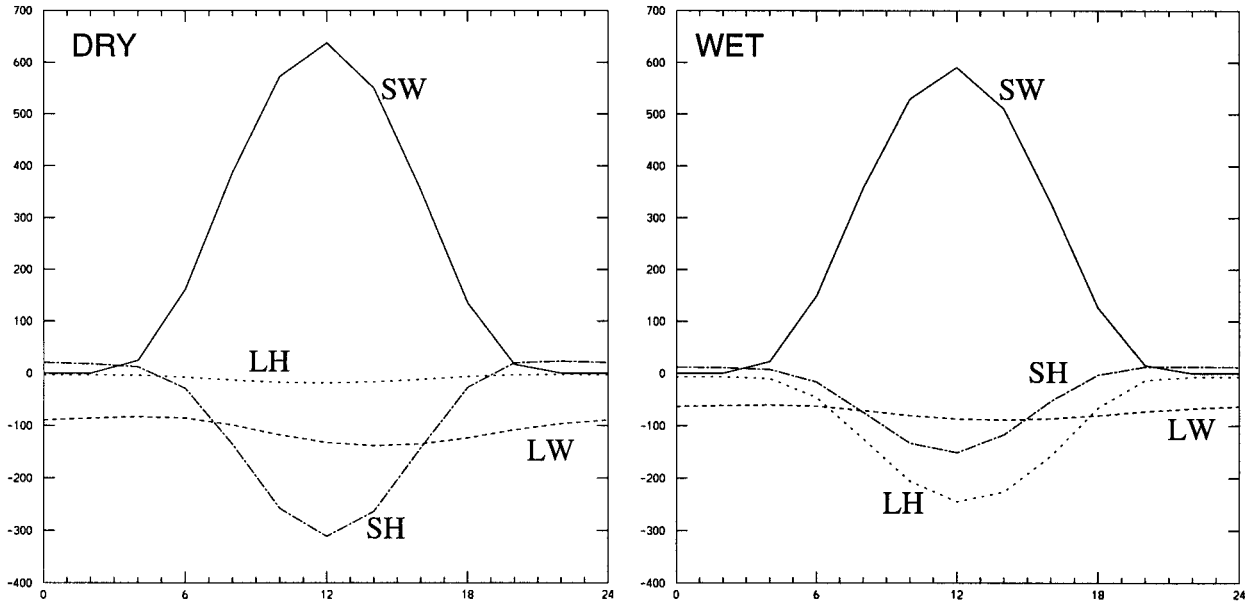

FIG. 15. Monthly mean diurnal cycle of the components of the surface energy balance (in W m^{-2}) with sensible heat (SH), latent heat (LH), net longwave (LW), and shortwave (SW) contributions.

there is a reduction of shortwave absorption associated with increased cloud cover, this effect is overpowered by LW radiative effects, yielding a higher net radiative energy flux over moist soil (and in cloudier conditions) than over dry soil (and in sunnier conditions). Thus, more energy is available over moist soils for the heating and moistening of the planetary boundary layer. Both of these factors can contribute toward increasing the boundary layer moist entropy and thus the potential for convective instability.

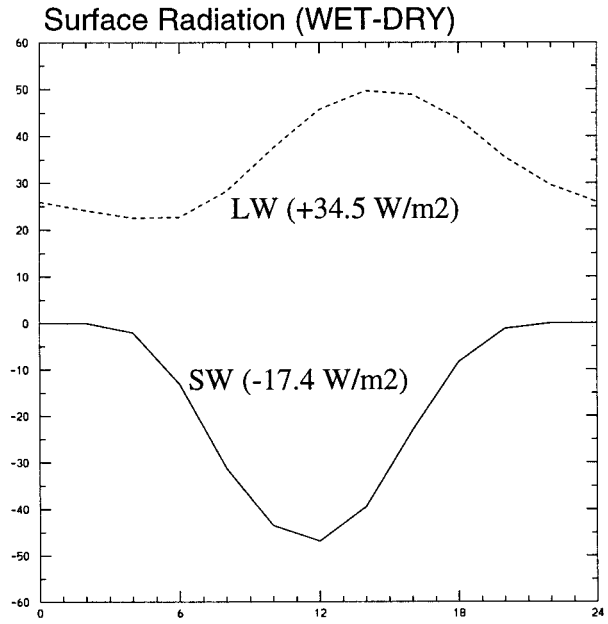

FIG. 16. Monthly mean diurnal cycle of the difference WET − DRY for the net SW and LW components of the surface energy balance (in W m^{-2}).

8. Conclusions

Month-long regional climate simulations were utilized to assess the sensitivity of the European summertime precipitation climate to prevailing soil moisture conditions. The results suggest, in qualitative agreement with the earlier study of Rowntree and Bolton (1983), that the soil moisture distribution has important implications for the summertime European precipitation distribution. In general, higher levels of soil moisture and evapotranspiration lead to higher levels of precipitation. The sensitivity of this effect is strongest in a belt between the wet Atlantic and the dry Mediterranean climate. As a result, the boundary between these two climatic regimes may be shifted by many hundreds of kilometers depending upon the underlying soil moisture conditions. The extent to which this process is important for the summertime interannual variability is, however, difficult to assess since the variability of the soil moisture on continental scales is not readily available with sufficient accuracy.

Although continental-scale modifications of the Bowen ratio imply some changes in the dynamical fields, the European soil–precipitation feedback is not of a large-scale dynamical nature (as might be the case for some deserts; see Charney 1975). Also, as we have demonstrated by means of detailed budget analyses, the feedback cannot be interpreted in terms of precipitation recycling, since recycling is far too inefficient on the spatial scales that matter in the European context, a

results which could have been anticipated in light of earlier studies on precipitation recycling (Budyko 1974; Brubaker 1993). The conclusion that emerges from our study thus is the following: The surplus of precipitation over wet as compared to dry soils derives primarily from atmospheric advection, and the soil–precipitation feedback relies on the sensitivity of the convective precipitation processes. The surplus of precipitation that falls over wet soils would thus, over dry soils, simply be advected across the domain of interest.

For the analysis of the mesoscale dynamical mechanisms, consideration was given to the mean diurnal cycle over selected subdomains. This technique has served to isolate the following three contributions. First, wet soils and low Bowen ratios lead to the buildup of shallow boundary layers. This concentrates the moist entropy flux into a shallow layer and thereby arrives at high values of convective available potential energy. Second, low Bowen ratios also imply high values of the relative humidity, thus lowering the level of free convection. Our simulation of these two factors agrees well with the discussion presented in Betts et al. (1996), who argued that the entrainment of free tropospheric air into the growing boundary layer will ultimately control the potential for convective instability. Third, the analysis of the surface energy balance did reveal the presence of a pronounced positive feedback mechanism of radiative origin. This radiative feedback is based upon the fact that the simulated net radiative flux (which ultimately can be converted into low-level moist entropy and convective instability) is larger over moist soils, in spite of the increased cloud cover. This result is consistent with a very recent observational study of Eltahir (1998).

The pronounced sensitivity in Europe, in a geographical region between the wet Atlantic and dry Mediterranean climate, is consistent with the aforementioned mechanism and the presence of weak synoptic-scale forcing. The synoptic-scale forcing provides the large-scale destabilization and moisture supply, while evapotranspiration determines the low-level relative humidity and moist entropy conditions. Consistent with this interpretation, we found that the soil–precipitation feedback over Europe is primarily a summertime feature. Similar sensitivity experiments for other months (April, October, January) revealed very weak sensitivity to soil conditions.

It should not be overlooked that several of the crucial processes that participate in the soil–precipitation feedback are of small scale and, thus, must be parameterized at the employed numerical resolution. Particularly critical aspects include the buildup of the diurnal boundary layer in response to solar heating, the release of moist convective instability, the associated formation of falling precipitation, and the feedback between cloud and radiative processes. The parameterization of these processes must currently be considered as uncertain. As a result, our model simulations must be considered with some caution, at least concerning the strength of the simulated feedback mechanism. This is particularly the case with respect to cloud–radiative feedbacks, which are key factors in determining the soil–precipitation sensitivity. Substantial sensitivity of the precipitation response with respect to the cloud–radiation feedback have also been noted with other numerical models, for instance with the MM4/RegCM regional climate model (J. Pal 1997, personal communication).

Despite the aforementioned difficulties, the key results of our study appear plausible, at least to the extent that our analysis has revealed a dynamically and physically highly consistent picture. Clearly, the validation (or falsification) of our results with observations would be highly desirable. Such a validation could for instance come from correlations of the atmospheric boundary layer structure and the surface energy balance with preceding soil moisture conditions. Some aspects might also be assessed by using estimates of the recycling rate as derived from the isotopic composition of precipitation and atmospheric vapor.

Provided that the strength of the simulated soil–precipitation feedback is approximately correct, some far-reaching conclusions about the European summer climate can be drawn: First, the soil moisture plays a fundamental role in the initial conditions of weather forecasting models, a feature that is well recognized at several forecasting centers. Improved operational assimilation schemes for soil moisture are badly needed in this area. Second, the presence of a strong soil–precipitation feedback in conjunction with the persistence of soil-moisture anomalies opens additional clues for seasonal forecasting. Here further work is needed about the predictability of precipitation anomalies in response to soil-moisture anomalies. Third, the sensitivity of the soil–precipitation feedback also implies that soil–atmosphere feedback processes require particular attention in the assessment of climate change.

Acknowledgments. We are indebted to the German Weather Service and the Swiss Meteorological Institute for providing access to the numerical model. Special thanks are due to Detlev Majewski (DWD) and to Jean Quiby (SMA) and their groups for technical support. We have benefited substantially from discussions with and comments from Uwe Böhm, Huw Davies, Elfatih Eltahir, Kerry Emanuel, Seita Emori, Dara Enthekabi, Pamela Heck, Martin Miller, Mitch Moncrieff, Atsumu Ohmura, Dave Raymond, Willi Schmid, Pedro Viterbo, and Heini Wernli. We also appreciate useful comments from one anonymous reviewer that contributed to improving the manuscript. The research was supported by a contribution of the Swiss Priority Program (Contract SPP-U 5001-44602).

REFERENCES

Alestalo, M., 1983. The atmospheric water vapour budget over Europe. *Variations in the Global Water Budget*, A. Street-Perrott et al., Eds., D. Reidel, 67–79.

Beljaars, A. C. M., P. Viterbo, M. J. Miller, and A. K. Betts, 1996: The anomalous rainfall over the United States during July 1993: Sensitivity to land surface parameterization and soil-moisture anomalies. *Mon. Wea. Rev.*, **124,** 362–383.

Betts, A. K., and J. H. Ball, 1995: The FIFE surface diurnal cycle climate. *J. Geophys. Res.*, **100,** 25 679–25 693.

——, ——, A. C. M. Beljaars, M. J. Miller, and P. A. Viterbo, 1996: The land surface–atmosphere interaction: A review based on observational and global modeling perspectives. *J. Geophys. Res.*, **101,** 7209–7225.

Brubaker, K. L., D. Enthekabi, and P. S. Eagleson, 1993: Estimation of continental precipitation recycling. *J. Climate,* **6,** 1077–1089.

Budyko, M. I., 1974: *Climate and Life.* Academic Press, 508 pp.

Burde, G. I, A. Zangvil, and P. J. Lamb, 1996: Estimating the role of local evaporation in precipitation for a two-dimensional region. *J. Climate,* **9,** 1328–1338.

Charney, J. G., 1975: Dynamics of deserts and drought in the Sahel. *Quart. J. Roy. Meteor. Soc.*, **101,** 193–202.

Claussen, M., 1997: Modeling bio-geophysical feedbacks in the African and Indian monsoon region. *Climate Dyn.*, **13,** 247–257.

Copeland, J. H., R. A. Pielke, and T. G. F. Kittel, 1996: Potential climatic impacts of vegetation change: A regional modeling study. *J. Geophys. Res.*, **101,** 7409–7418.

Cress, A., D. Majewski, R. Podzun, and V. Renner, 1995: Simulation of European climate with a limited area model. Part I: Observed boundary conditions. *Contrib. Atmos. Phys.*, **68,** 161–178.

Davies, H. C., 1976: A lateral boundary formulation for multi-level prediction models. *Quart. J. Roy. Meteor. Soc.*, **102,** 405–418.

Dickinson, R. E., 1984: Modeling evapotranspiration for three-dimensional global climate models. *Climate Processes and Climate Sensitivity, Geophys. Monogr.,* No. 29, Amer. Geophys. Union, 58–72.

——, and A. Henderson-Sellers, 1988: Modelling tropical deforestation: A study of GCM land–surface parameterizations. *Quart. J. Roy. Meteor. Soc.*, **114,** 439–462.

DWD, 1995: Dokumentation des EM/DM—Systems. 492 pp. [Available from German Weather Service, Zentralamt, 63004 Offenbach am Main, Germany.]

——, 1997: Quarterly report of the operational NWP-models of the Deutscher Wetterdienst. [Available from German Weather Service, Zentralamt, 63004 Offenbach am Main, Germany.]

Eltahir, E. A. B., 1998: A soil moisture rainfall feedback mechanism: 1: Theory and observations. *Water Resour. Res.*, **34,** 765–776.

——, and R. L. Bras, 1994: Precipitation recycling in the Amazon basin. *Quart. J. Roy. Meteor. Soc.*, **120,** 861–922.

——, and J. S. Pal, 1996: Relationship between surface conditions and subsequent rainfall in convective storms. *J. Geophys. Res.*, **101,** 26 237–26 245.

Enthekabi, D., 1995: Recent advances in land–atmosphere interaction research. *Rev. Geophys.,* Supplement ''U.S. National Report to International Union of Geodesy and Geophysics, 1991–1994,'' 995–1003.

——, I. Rodriguez-Iturbe, and R. L. Bras, 1992: Variability in large-scale water balance with land surface–atmosphere interaction. *J. Climate,* **5,** 798–813.

Findell, K. L., and E. A. B. Eltahir, 1997: An analysis of the relationship between spring soil moisture and summer rainfall, based on direct observations from Illinois. *Water Resour. Res.*, **33,** 725–735.

Frei, C., C. Schär, D. Lüthi, and H. C. Davies, 1998: Heavy precipitation processes in a warmer climate. *Geophys. Res. Lett.*, **25,** 1431–1434.

Giorgi, F., L. O. Mearns, C. Shields, and L. Mayer, 1996: A regional model study of the importance of local versus remote controls of the 1988 drought and the 1993 flood over the Central United States. *J. Climate,* **9,** 1150–1162.

Jacobsen, I., and E. Heise, 1982: A new economic method for the computation of the surface temperature in numerical models. *Beitr. Phys. Atmos.*, **55,** 128–141.

Joussaume, S., J. Jouzel, and R. Sadourny, 1984: A general circulation model of water isotope cycles in the atmosphere. *Nature,* **311** 24–29.

Jouzel, J., K. Froehlich, and U. Schotterer, 1997: Deuterium and oxygen-18 in present-day precipitation: Data and modelling. *Hydrol. Sci. J.,* **42,** 747–763.

Kalnay, E., and Coauthors, 1996: The NCEP/NCAR 40-Year Reanalysis Project. *Bull. Amer. Meteor. Soc.*, **77,** 437–471.

Koster, R., J. Jouzel, R. Suozzo, and G. Russell, 1986: Global sources of local precipitation as determined by the NASA/GISS GCM. *Geophys. Res. Lett.*, **13,** 121–124.

Lean, J., and P. R. Rowntree, 1993: A GCM simulation of the impact of Amazonian deforestation on climate using an improved canopy representation. *Quart. J. Roy. Meteor. Soc.*, **119,** 509–530.

Louis, J. F., 1979: A parametric model of vertical eddy fluxes in the atmosphere. *Bound.-Layer Meteor.*, **17,** 187–202.

Lüthi, D., A. Cress, H. C. Davies, C. Frei, and C. Schär, 1996: Interannual variability and regional climate simulations. *Theor. Appl. Climatol.*, **53,** 185–209.

Mahfouf, J.-F., 1991: Analysis of soil moisture from near-surface parameters. A feasibility study. *J. Appl. Meteor.*, **30,** 1534–1547.

Majewski, D., 1985: Balanced initial and boundary values for a limited-area model. *Contrib. Atmos. Phys.*, **58,** 147–159.

——, 1991: The Europa-Modell of the Deutscher Wetterdienst. *Proc. Seminar on Numerical Methods in Atmospheric Models,* Reading, United Kingdom, ECMWF, 147–191.

McDonald, J. E., 1962: The evapotranspiration–precipitation fallacy. *Weather,* **17,** 168–177.

Mellor, G. L., and T. Yamada, 1974: A hierarchy of turbulence closure models for planetary boundary layers. *J. Atmos. Sci.*, **31,** 1791–1806.

Monteith, J. L., 1981: Evaporation and surface temperature. *Quart. J. Roy. Meteor. Soc.*, **107,** 1–27.

Müller, E., 1981: Turbulent flux parameterization in a regional-scale model. *Proc. Workshop on Planetary Boundary Layer Parameterization,* Reading, United Kingdom, ECMWF, 193–220.

Oglesby, R. J., and D. J. Erickson, 1989: Soil moisture and the persistence of North American drought. *J. Climate,* **2,** 1362–1380.

Rind, D., 1982: The influence of ground moisture conditions in North America on summer climate as modeled with the GISS GCM. *Mon. Wea. Rev.*, **110,** 1487–1494.

Ritter, B., and J. F. Geleyn, 1992: A comprehensive radiation scheme for numerical weather prediction with potential applications in climate simulations. *Mon. Wea. Rev.*, **120,** 305–325.

Rowntree, P. R., and J. A. Bolton, 1983: Simulations of the atmospheric response to soil moisture anomalies over Europe. *Quart. J. Roy. Meteor. Soc.*, **109,** 501–526.

Schär, C., C. Frei, D. Lüthi, and H. C. Davies, 1996: Surrogate climate change scenarios for regional climate models. *Geophys. Res. Lett.*, **23,** 669–672.

Shukla, J., and Y. Mintz, 1982: Influence of land–surface evapotranspiration on the earth's climate. *Science,* **215,** 1498–1501.

Simmonds, I., and P. Hope, 1997: Persistence characteristics of Australian rainfall anomalies. *Int. J. Climatol.*, **17,** 597–613.

Tiedtke, M., 1989: A comprehensive mass flux scheme for cumulus parameterization in large-scale models. *Mon. Wea. Rev.*, **117,** 1779–1800.

Viterbo, P., 1995: Initial values of soil water and the quality of summer forecasts. *ECMWF Newslett.*, **69,** 2–8.

Williams, E., and N. Renno, 1993: An analysis of the conditional instability of the tropical atmosphere. *Mon. Wea. Rev.*, **121,** 21–36.

Yeh, T.-C., R. T. Wetherald, and S. Manabe, 1984: The effect of soil moisture on the short-term climate and hydrology change—A numerical experiment. *Mon. Wea. Rev.*, **112,** 474–490.